Article

Two-Dimensional Supramolecular Nanopatterns Formed by the Coadsorption of Guanine and Uracil at the Liquid/Solid Interface

Wael Mamdouh, Ross E. A. Kelly, Mingdong Dong, Lev N. Kantorovich, and Flemming Besenbacher

J. Am. Chem. Soc., **2008**, 130 (2), 695-702 • DOI: 10.1021/ja076832f

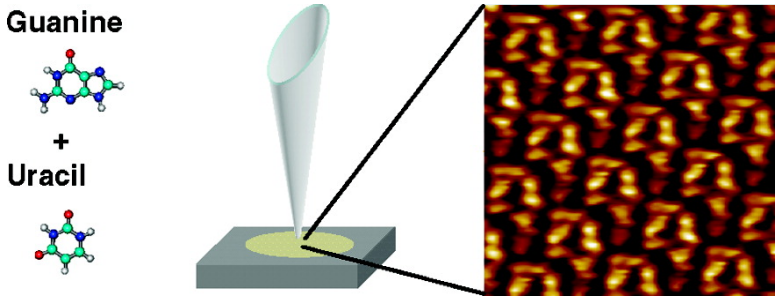

J|A|C|S
ARTICLES
Published on Web 12/12/2007

Two-Dimensional Supramolecular Nanopatterns Formed by the Coadsorption of Guanine and Uracil at the Liquid/Solid Interface

Wael Mamdouh,*,† Ross E. A. Kelly,‡,§ Mingdong Dong,† Lev N. Kantorovich,‡ and Flemming Besenbacher*,†

Interdisciplinary Nanoscience Center (iNANO), Centre for DNA Nanotechnology (CDNA), and Department of Physics and Astronomy, University of Aarhus, DK-8000 Arhus C, Denmark, Department of Physics, School of Physical Sciences and Engineering, King's College London, Strand, London, U.K. WC2R 2LS, and Department of Physics and Astronomy, University College London, Gower Street, London, U.K. WC1E 6BT

Received September 10, 2007; E-mail: wael@inano.dk; fbe@inano.dk

Abstract: A novel supramolecular nanostructure formed by the coadsorption of the complementary nucleobases guanine (G) and uracil (U) at the liquid (1-octanol solvent)/solid (graphite) interface is revealed by scanning tunneling microscopy (STM). The GU supramolecular structure is distinctly different from the structures observed by STM when the individual nucleobases (NB) are adsorbed on graphite in the control experiments. Using a systematic methodology and ab initio density functional theory (DFT), an atomistic structural model is proposed for the supramolecular coadsorbed GU structure, which consists of a periodic repetition of cyclic units based on the strongest GU base pairing.

1. Introduction

DNA and RNA play a pivotal role in biological processes due to their ability to store and reproduce genetic information. DNA and RNA nucleobase (NB) pairing via hydrogen bonding underlies the transfer of genetic information in many biological processes,[1] plays an important role in many novel biosensors based on surface functionalization with ss-DNA oligomers,[2] and has also been used to steer the self-assembly of DNA-based artificial molecular constructions.[3] It has recently been demonstrated that DNA/RNA are also unique biomolecules suitable for the design and formation of self-assembled nanostructures since it is possible to use their base sequences to encode instructions for assembly in a predetermined fashion at the nanometer scale.[4] In this context, simplified model systems, where the NB molecules are removed from the DNA/RNA backbone, are of great importance and have recently been pursued both experimentally[5] and theoretically.[6] Additionally, it is of great fundamental importance to study self-assemblies of NB molecules as means to explore their *inter*- and *intra*-molecular hydrogen-bonding properties and their ability to bind to proteins, amino acids, and more complex biological systems, which may lead to supramolecular nanoscale structures.[7]

The unique capability of scanning probe microscopy (SPM) to explore the atomic-scale realm of matter and in particular to directly observe individual NB molecules has allowed novel insights into how DNA NB molecules interact with each other and how they may form functional nanoscale assemblies.[8,9] Recently, a variety of STM studies on surface supramolecular structures formed by individual NB molecules have been reported.[10−14] These studies range from pioneering studies in

† University of Aarhus.
‡ King's College London.
§ University College London.

(1) (a) Watson, J. D.; Crick, F. H. C. *Nature* **1953**, *171*, 737−738. (b) Saenger, W. *Principles of Nucleic Acid Structure*; Springer: Berlin, 1984.
(2) (a) Taton, T. A.; Mirkin, C. A.; Letsinger, R. L. *Science* **2000**, *289*, 1757−1760. (b) Fritz, J.; Baller, M. K.; Lang, H. P.; Rothuizen, H.; Vettiger, P.; Meyer, E.; Guntherodt, H. J.; Gerber, C.; Gimzewski, J. K. *Science* **2000**, *288*, 316−318.
(3) (a) Samorì, B.; Zuccheri, G. *Angew. Chem., Int. Ed.* **2005**, *44*, 1166−1181. (b) Sessler, J. L.; Jayawickramarajah, J. *Chem. Commun.* **2005**, 1939−1949. (c) Seeman, N. C. *Angew. Chem., Int. Ed.* **1998**, *37*, 3220−3238.
(4) (a) Gothelf, K. V.; LaBean, T. H. *Org. Biomol. Chem.* **2005**, *3*, 4023−4037. (b) Yan, H.; Park, S. H.; Finkelstein, G.; Reif, J. H.; LaBean, T. H. *Science* **2003**, *301*, 1882−1884. (c) Mao, C. D.; LaBean, T. H.; Reif, J. H.; Seeman, N. C. *Nature* **2000**. (d) Yan, H.; Feng, L. P.; LaBean, T. H.; Reif, J. H. *J. Am. Chem. Soc.* **2003**, *125*, 14246−14247.
(5) (a) Nir, E.; Kleinermanns, K.; de Vries, M. S. *Nature* **2000**, *408*, 949−951. (b) Guerra, C. F.; Bickelhaupt, F. M.; Snijders, J. G.; Baerends, E. J. *J. Am. Chem. Soc.* **2000**, *122*, 4117−4128. (c) Abo-Riziq, A.; Grace, L.; Nir, E.; Kabelac, M.; Hobza, P.; de Vries, M. S. *Proc. Natl. Acad. Sci. U.S.A.* **2005**, *102*, 20−23.
(6) (a) Guerra, C. F.; Bickelhaupt, F. M. *Angew. Chem., Int. Ed.* **1999**, *38*, 2942−2945. (b) Blancafort, L.; Bertran, J.; Sodupe, M. *J. Am. Chem. Soc.* **2004**, *126*, 12770−12771. (c) Grunenberg, J. *J. Am. Chem. Soc.* **2004**, *126*, 16310−16311. (d) Gorb, L.; Podolyan, Y.; Dziekonski, P.; Sokalski, W. A.; Leszczynski, J. *J. Am. Chem. Soc.* **2004**, *126*, 10119−10129.
(7) Chen, Q.; Richardson, N. V. *Nat. Mater.* **2003**, *2*, 324−328.
(8) Xu, S.; Dong, M.; Rauls, E.; Otero, R.; Linderoth, T. R.; Besenbacher, F. *Nanolett.* **2006**, *6*, 1434−1438.
(9) (a) Rabe, J. P.; Buchholz, S. *Science* **1991**, *253*, 424−427. (b) Cyr, D. M.; Venkataraman, B.; Flynn, G. W. *Chem. Mat.* **1996**, *8*, 1600−1615. (c) Berg, A. M.; Patrick, D. L. *Angew. Chem., Int. Ed.* **2005**, *44*, 1821−1823. (d) Qiu, X. H.; Wang, C.; Zeng, Q. D.; Xu, B.; Yin, X. S.; Wang, H. N.; Xu, S. D.; Bai, C. L. *J. Am. Chem. Soc.* **2000**, *122*, 5550−5556. (e) De Feyter, S.; De Schryver, F. C. *Chem. Soc. Rev.* **2003**, *32*, 139−150. (f) Cai, Y. G.; Bernasek, S. L. *J. Am. Chem. Soc.* **2004**, *126*, 14234−14238. (g) Katsonis, N.; Marchenko, A.; Fichou, D. *J. Am. Chem. Soc.* **2003**, *125*, 13682−13683.
(10) (a) Kelly, R. E. A.; Kantorovich, L. N. *J. Mater. Chem.* **2006**, *16*, 1894−1905. (b) Kelly, R. E. A.; Kantorovich, L. N. *Surf. Sci.* **2005**, *589*, 139−152. (c) Shinoda, K.; Shinoda, W.; Liew, C. C.; Tsuzuki, S.; Morikawa, Y.; Mikami, M. *Surf. Sci.* **2004**, *556*, 109. (d) Mamdouh, W.; Dong, M.; Kelly, R. E. A.; Kantorovich, L. N.; Besenbacher, F. *J. Phys. Chem. B* **2007**, *111*, 12048.

air,[11g,h,14b−e] demonstrating self-assembly of NB molecules into two-dimensional (2D) ordered structures upon solvent evaporation, to detailed low-temperature ultrahigh vacuum (UHV) STM studies,[14c,g] revealing nucleation through the formation of NB molecular dimers. Additionally, more complex structures have been investigated, such as networks consisting of a honeycomb arrangement of guanine (G) derivatives[14c] or G quartets.[13] However, coadsorption experiments,[15] designed to investigate the complementary interaction between *different* kinds of NB molecules with local probe techniques, are still rather scarce. Tanaka and Kawai were capable of discriminating individual thymine (T) and adenine (A) NB molecules in STM images after depositing T on A adlayers on a $SrTiO_3$ surface.[15c] Furthermore, STM studies of self-assemblies of complementary NB molecules A and T on highly ordered pyrolytic graphite (HOPG) surfaces show the formation of 2D supramolecular cyclic network structures, consisting of reverse Hoogsteen ATAT-quartets separated by adenine chains.[16] Similarly, the complementary NB molecules G and cytosine (C) also form a nanopatterned surface structure, but this one consists of GC Watson−Crick base pairing.[8]

A similar study involving the self-assembly of the complementary RNA bases A and uracil (U) revealed aperiodic structures on HOPG.[16] Another very important NB pairing is that between G and U. In particular, the Wobble configuration (G-U and inosine (I)-U/I-A/I-C) is fundamental in the RNA secondary structure, and is critical for the translation of the genetic code. The GU Wobble configuration has unique chemical, structural, dynamic, and ligand-binding properties[17] and contains suitable sites for recognition by proteins and other RNAs. The GU Wobble configuration also constitutes the most common mismatch in the helices of rRNA and tRNA as it provides recognition signals for autoregulation of protein synthesis and has the ability to bind divalent metal ions, which is important for RNA catalysis.

Here we have studied the self-assembly of G and U NB molecules individually, and the coadsorption of G and U, respectively, at the liquid−solid interface by STM. In the control experiments, where the individual G and U NB molecules are adsorbed separately at the graphite surface, the structures observed are dominated by dimer formation. Interestingly, after mixing the two complementary NB molecules G and U, new cyclic structures which are significantly different from the structures obtained by the pure NB molecules are observed. To gain further insight into the nature and composition of these cyclic coadsorbed structures, a systematic methodology is used to determine the G-U superstructures followed by ab initio DFT calculations and a subsequent detailed comparison with the experimental STM images. We find that the fundamental building blocks are GU NB dimers that form one-dimensional (1D) GU chains and that further bind via hydrogen bonding, resulting in the 2D GU monolayers.

2. Experimental and Computational Section

The STM experiments were performed at the liquid (1-octanol)/solid (HOPG)) interface under ambient conditions at room temperature using a MultiMode SPM system with a Nanoscope IIIa controller (Veeco Instruments Inc., Santa Barbara, CA). STM tips were mechanically cut from a 0.25 mm Pt/Ir (80/20)% wire and tested on freshly cleaved HOPG surfaces (HOPG, grades ZYA and ZYB, Advanced Ceramics Inc., Cleveland, OH and NT-MDT, respectively). Prior to imaging, guanine (G) (Sigma Aldrich, 98% purity) and uracil (U) (Sigma Aldrich, 99% purity) were dissolved separately in 1-octanol (Sigma Aldrich, 99.5% purity) at a concentration of 1.0 mg/g for G and 0.8 mg/g for U, respectively, and a drop of one of the solutions was applied onto a freshly cleaved surface of HOPG to form either G or U structures. To prepare the (G + U) mixture, we mixed the solutions of G dissolved in 1-octanol with the solution of U dissolved in 1-octanol (with 1:1 mixing molar ratio), and one drop of the G + U mixture was applied onto a freshly cleaved HOPG surface. Then the STM tip was immersed in any of the solutions, and images were recorded at the 1-octanol/graphite interface.

Several tips and HOPG samples were used to ensure that reproducible results were obtained and to avoid any artifacts related to the STM imaging. The STM images were recorded in constant-current mode. For a proper unit cell calibration of the G and U STM recorded structures, the recording of the molecular STM images were subsequently followed by imaging the underlying graphite substrate under the same experimental conditions, apart from lowering the bias voltage. The STM images were analyzed using scanning probe image processor (SPIP) software program (Image Metrology ApS, Lyngby, Denmark),[18] and the STM images were corrected for any drift using the recorded graphite calibration images, which allowed us to determine the unit cells accurately. Furthermore, the correlation averaging method[19] was applied to the STM images in A and B of Figure 1 and B of Figure 2 for more detailed image analysis and for the display of the high-resolution STM images. The STM image in Figure 1B has been rotated 90° for display purposes. We always investigated very thoroughly that this method did not affect the unit cell parameters. The imaging parameters (the tunneling current, I_{tunn}, and the sample bias voltage, V_{bias}) are stated in the figure captions.

(11) (a) Perdigão, L. M. A.; Staniec, P. A.; Champness, N. R.; Kelly, L. N. Kantorovich, R. E. A.; Beton, P. H. *Phys. Rev. B* **2006**, *73*, 195423. (b) Tanaka, H.; Kawai, T. *Jpn. J. Appl. Phys.* **1996**, *35*, 3759−3763 (Part 1, No. 6B). (c) Furukawa, M.; Tanaka, H.; Kawai, T. *Surf. Sci.* **1997**, *392*, L33−L39. (d) Tanaka, H.; Yoshinobu, J.; Kawai, M.; Kawai, T. *Jpn. J. Appl. Phys.* **1996**, *35*, L244−L246 (Part 2, No. 2B). (e) Nakagawa, T.; Tanaka, H.; Kawai, T. *Surf. Sci.* **1997**, *770*, L144−L148. (f) Freund, J. E.; Edelwirth, M.; Krobel, P.; Heckl, W. M. *Phys. Rev. B* **1997**, *55*, 5394−5397. (g) Heckl, W. M.; Smith, D. P. E.; Binnig, G.; Klagges, H.; Hänsch, T. W.; Maddocks, J. *Proc. Natl. Acad. Sci. U.S.A.* **1991**, *88*, 8003−8005. (h) Allen, M. J.; Balooch, M.; Subbiah, S.; Tenth, R. J.; Siekhaus, W.; Barlhorn, R. *Scanning Microsc.* **1991**, *5*, 625−630.
(12) (a) Tao, N. J.; Shi, Z. *J. Phys. Chem.* **1994**, *98*, 1464−1471. (b) Srinivasan, R.; Murphy, J. C. *Ultramicroscopy* **1992**, *42*−*44*, 453−459. (c) Sowerby, S. J.; Edelwirth, M.; Heckl, W. M. *J. Phys. Chem. B* **1998**, *102*, 5914−5922. (d) Dretschkow, Th.; Dakkouri, A. S.; Wandlowski, Th. *Langmuir* **1997**, *13*, 2843−2856. (e) Sowerby, S. J.; Heckl, W. M.; Petersen, G. B. *J. Mol. Evol.* **1996**, *43*, 419−424. (f) Edelwirth, M.; Freund, J.; Sowerby, S. J.; Heckl, W. M. *Surf. Sci.* **1998**, *417*, 201−209. (g) Sowerby, S. J.; Petersen, G. B. *J. Electroanal. Chem.* **1997**, *433*, 85−90. (h) Sowerby, J.; S.; Edelwirth, M.; Heckl, W. M. *Appl. Phys. A* **1998**, *66*, S649−S653.
(13) Otero, R.; Schöck, M.; Molina, L. M.; Lægsgaard, E.; Stensgaard, I.; Hammer, B.; Besenbacher, F. *Angew. Chem., Int. Ed.* **2005**, *44*, 2270−2275.
(14) (a) Boland, T.; Ratner, B. D. *Langmuir* **1994**, *10*, 3845−3852. (b) Furukawa, M.; Tanaka, H.; Kawai, T. *J. Chem. Phys.* **2001**, *115*, 3419−3423. (c) Giorgi, T.; Lena, S.; Mariani, P.; Cremonini, M. A.; Masiero, S.; Pieraccini, S.; Rabe, J. P.; Samori, P.; Spada, G. P.; Gottarelli, G. *J. Am. Chem. Soc.* **2003**, *125*, 14741−14749. (d) Gottarelli, G.; Masiero, S.; Mezzina, E.; Pieraccini, S.; Rabe, J. P.; Samori, P.; Spada, G. P. *Chem.-Eur. J.* **2000**, *6*, 3242−3248. (e) Furukawa, M.; Tanaka, H.; Kawai, T. *Surf. Sci.* **2000**, *445*, 1−10. (f) Sowerby, S. J.; Stockwell, P. A.; Heckl, W. M.; Petersen, G. B. *Origins. Life Evol. Biosphere* **2000**, *30*, 81−99. (g) Srinivasan, R.; Murphy, J. C.; Fainchtein, R.; Pattibiraman, N. *J. Electroanal. Chem.* **1991**, *312*, 293−300. (h) Tao, N. J.; Derose, J. A.; Lindsay, S. M. *J. Phys. Chem.* **1993**, *97*, 910−919.
(15) (a) Camargo, A. P. M.; Baumgartel, H.; Donner, C. *Phys. Chem. Chem. Phys.* **2003**, *5*, 1657−1664. (b) Kirste, S.; Donner, C. *Phys. Chem. Chem. Phys.* **2001**, *3*, 4384−4389. (c) Tanaka, H.; Kawai, T. *Mater. Sci. Eng. C* **1995**, *3*, 143−148.
(16) Mamdouh, W.; Dong, M.; Xu, S.; Rauls, E.; Besenbacher, F. *J. Am. Chem. Soc.* **2006**, *128*, 13305−13311.
(17) Varani, G. H.; McClain, W. *EMBO Rep.* **2000**, *1*, 18−23.
(18) http://www.imagemet.com.
(19) Samorí, P.; Engelkamp, H.; de Witte, P.; Rowan, A. E.; Note, R. J. M.; Rabe, J. P. *Angew. Chem.* **2001**, *113*, 2410−2412; *Angew. Chem., Int. Ed.* **2001**, *40*, 2348−2350.

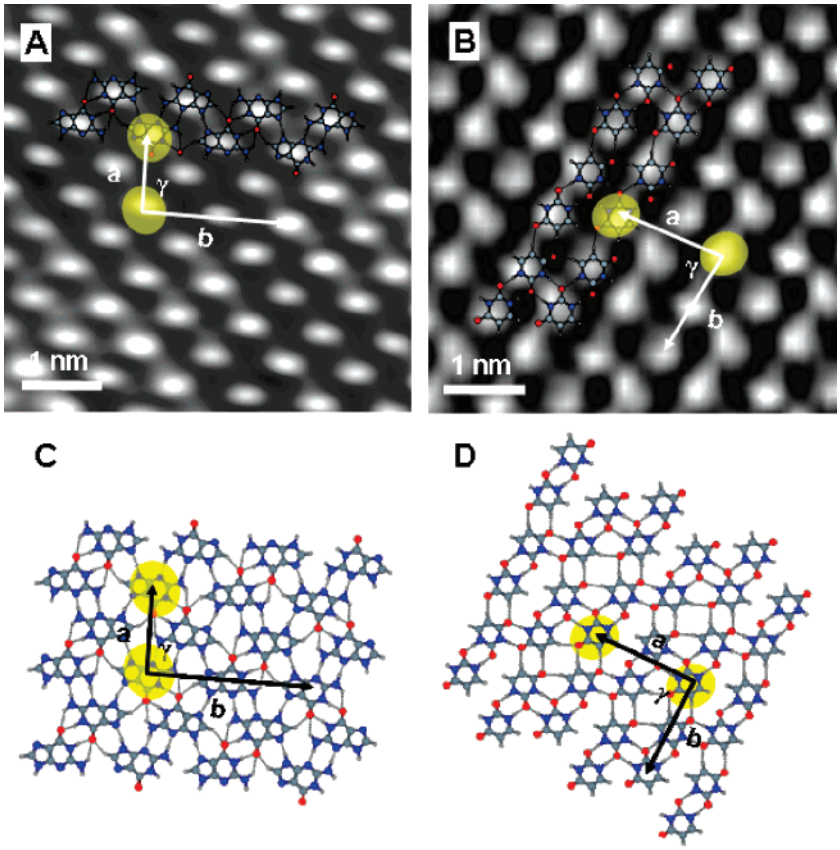

Figure 1. High-resolution STM images of guanine (G) and uracil (U) self-assemblies at the 1-octanol/graphite interface. (A) G, tunneling parameters are $I_{tunn} = 0.76$ nA, $V_{bias} = 550$ mV. (B) U, tunneling parameters are $I_{tunn} = 1.69$ nA, $V_{bias} = -753.5$ mV, respectively. (C,D) gas-phase ab initio DFT calculated structures proposed to explain the observed STM images in A and B, respectively. The unit cells are explicitly indicated. The stability of each unit cell (consisting of four bases) is −5.09 and −3.33 eV for the G and U monolayers, respectively. For display purposes, individual molecules are indicated in yellow, and two parts of the calculated structures in C and D are superimposed on the STM images in A and B, respectively.

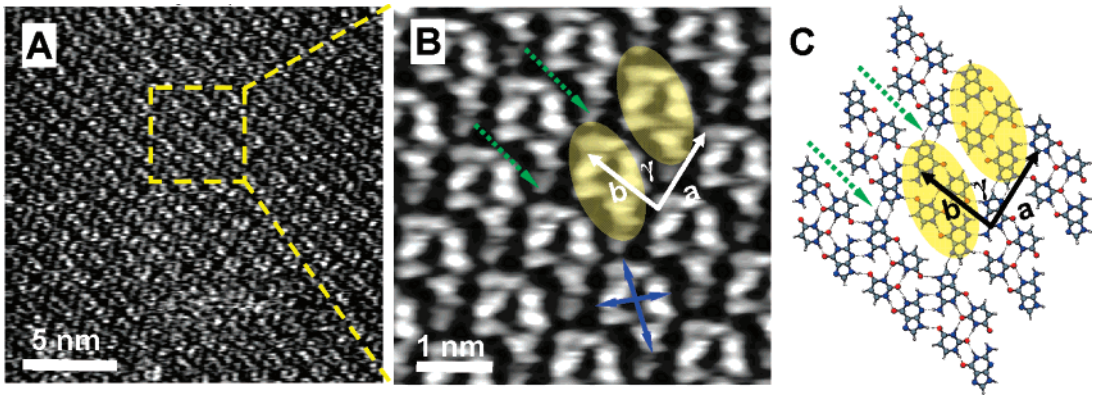

Figure 2. High-resolution STM images of GU-base pairs at the 1-octanol/graphite interface. (A) large-scale STM image, (B) zoom-in image of the yellow area indicated in A. Tunneling parameters are $I_{tunn} = 0.70$ nA, $V_{bias} = 589.0$ mV. (C) Molecular structure proposed by ab initio calculations. The GU-cyclic structures are indicated by yellow ovals, their size by blue arrows, and the unit cell lattice vectors are indicated. Green arrows indicate the hydrogen bonds between the GU-cyclic structures along unit cell vector ***a.*** The stability is −3.92 eV per unit cell (consisting of four bases).

Theoretical calculations of the super structures were performed in the gas phase using the ab initio DFT SIESTA method.[20,21] Briefly, SIESTA uses a localized numerical atomic orbital basis set, periodic boundary conditions, and the method of pseudopotentials. In all calculations, the DZP (double-ζ plus polarization orbitals) basis set was used with an appropriate energy cutoff of 10 meV. The large size of the basis set is essential in order to obtain realistic bonding between molecules. The Perdew, Becke, and Ernzerhof (PBE)[22] density functional was used for the exchange-correlation energy. Atomic relaxation was performed until the forces on each atom were not larger than 0.05 eV/Å. Note that no constraints were applied during the relaxations and that all structures relaxed into relatively planar configurations. Due to the large cell sizes in the calculations, the graphite surface was not included in the calculations, and only one (Γ) k-point was required for these calculations. The basis set superposition error (BSSE) corrections are essential to get reliable energetics in localized basis set calculations. These corrections have been calculated by the standard Boys−Bernardi

(20) Ordejon, P.; Artacho, E. and Soler, J. M. *Phys. Rev. B* **1996**, *53*, R10441−R10444.
(21) Soler, J. M.; Artacho, E.; Gale, J. D.; Garcia, A.; Junquera, J.; Ordejon, P. and D. Sanchez-Portal, *J. Phys.: Condens. Matter* **2002**, *14*, 2745−2779.
(22) Perdew, J. P.; Burke, K.; Ernzerhof, M. *Phys. Rev. Lett.* **1996**, *77*, 3865−3868.

Table 1. Lattice Parameters of the Nucleobases

	experimental			calculated		
nucleobases	**a** (nm)	**b** (nm)	γ (deg)	**a** (nm)	**b** (nm)	Γ (deg)
uracil	1.30 ± 0.10	1.20 ± 0.20	87 ± 2.5	1.25	1.22	86.3
guanine	1.04 ± 0.10	1.81 ± 0.18	93.2 ± 2.5	0.94	1.88	90.0
U + G	1.22 ± 0.10	1.27 ± 0.10	86.7 ± 2.0	1.34	1.35	83.9

counterpoise correction method.[23] This ab initio technique has been extensively tested for DNA and RNA homopairs[24] and a large selection of heteropairs[25] involving DNA and RNA bases by comparing with high-level quantum chemistry (QC) calculations.[26] The calculations reveal an excellent agreement with the benchmark results.[24,25]

3. Results and Discussion

3.1. STM Results. High-resolution STM images of adsorbed layers of G (Figure 1A) and U (Figure 1B) at the 1-octanol/graphite interface are shown, while the corresponding ab initio DFT calculations of the structures are depicted respectively in C and D of Figure 1. The unit cells of individual NB molecules are depicted in Figure 1, and, as can be seen, both G and U networks contain four molecules per unit cell, with the unit cell lattice parameters given in Table 1.

The high-resolution STM image of pure G (Figure 1A) reveals a quasi-square arrangement. In Figure 1C, a calculated molecular model for the 2D supramolecular G network based on the strongest G dimer[24b] is shown, and the model is seen to be in good agreement with both the 2D supramolecular G network observed in the STM image in Figure 1A as well as with a structural model proposed earlier, relaxed with less accurate semiclassical methods.[12c] It should be noted that a completely different G-network is observed on Au(111) under ultrahigh vacuum (UHV) conditions[13] where G molecules self-assembled into a structure based on the biologically relevant G-quartets. This quartet structure is stabilized by cooperative charge-transfer effects which strengthen the intermolecular hydrogen bonds within the G-quartets. Interestingly, the G monolayer network structure observed on HOPG is found to be by -0.13 eV per molecule more stable in the gas phase than the G quartet network. This difference is due to the fact that each G molecule inside the G monolayer shown in Figure 1C can interact with four G neighboring molecules (involving five hydrogen bonds of various strengths per molecule), whereas in the G quartet network every G molecule only forms connections with three molecules which corresponds to a total of three hydrogen bonds per molecule. Although one may expect a rather weak corrugation potential should be felt by the NBs on atomically flat surfaces such as Au(111)[13] and HOPG,[27] the fact that different G structures are favored on these surfaces means that the molecule−surface interaction is significant in these cases in providing different confining potentials.

On the other hand, the STM images of the pure U (Figure 1B) monolayer structure reveal bright rows corresponding to the U dimers aligned into adjacent parallel 1D chains. This suggestion is confirmed by DFT calculations, which reveal that a monolayer consisting of the energetically most favorable U dimer[24a] forms. These U dimer structures are in good agreement with previously proposed models of U crystalline lattices on the HOPG surface in air, which also form superstructures that have commensurate lattices with respect to the underlying substrate.[12g,h]

In Figure 2 high-resolution STM images of the coadsorbed GU-nanopattern structure physisorbed at the 1-octanol/graphite interface are shown. When the GU coadsorbed structure is compared with the structures observed by the pure G and U molecules as depicted in Figure 1, the well-ordered GU monolayer in Figure 2 is found to be significantly different from the homomolecular phase. In the observed mixed GU nanopattern, rows that contain "cyclic" structures, indicated by yellow ovals in Figure 2B, are clearly revealed, with dimensions of 1.00 ± 0.10 nm and 1.4 ± 0.10 nm, respectively, as indicated by blue arrows. In order to understand such a GU mixed structure, we have performed ab initio DFT calculations. These cyclic structures are also seen in the proposed molecular model depicted in Figure 2C which was relaxed using an ab initio DFT method.

In Table 1 we have compared the lattice parameters of the GU-cyclic structures determined experimentally with those calculated theoretically for the most suitable supramolecular models. It is also worth noting that semi-classical molecular dynamics (MD) calculations of the NB molecules on the graphite surface show a planar configuration with a slight tilting of the NB molecules with respect to the surface. This tilting may slightly increase the packing density of the molecules on the surface.[12h] However, such a minor tilting of the NB molecules cannot be resolved in the STM experiments presented here, which might be due to: (i) the presence of a liquid environment that allows some degree of freedom for the NB molecules to move freely on the surface and may therefore change their orientation and location on the surface regularly within a short time scale, (ii) the fact that these NB molecules are short and do not contain any side chains that could anchor them to the graphite surface during the scanning process, which again enhances their mobility on the surface, and (iii) the interplay between molecule−molecule versus molecule−substrate interaction is one of the key aspects in the self-assembly of organic molecules in general, and therefore, it is hard to predict which interaction is stronger than the other that will allow such a tilting process to occur and/or to be identified by STM, taking into account that the ab initio DFT calculations did not consider the surface of the graphite and its interaction with the NB molecules as pointed out previously.

Next we discuss how the interplay between the experimental findings and the theoretical calculations allowed us to determine the most favorable G-U structural model.

3.2. Ab Initio DFT calculations. We have used a systematic approach[10,11a] to reveal the supramolecular structures of the GU periodic nanostructures by initially identifying binding sites on the individual G and U NB molecules and then exploring how they can adjoin.

All possible binding sites which can participate in forming at least double hydrogen bonds between the NB molecules are explicitly indicated on the G and U molecules in Figure 3A.

(23) Boys, S. F.; Bernardi, F. *Mol. Phys.* **1970**, *19*, 553−566.
(24) (a) Kelly, R. E. A.; Kantorovich, L. N. *J. Phys. Chem. B* **2006**, *110*, 2249−2255. (b) Kelly, R. E. A.; Lee, Y. J.; Kantorovich, L. N. *J. Phys. Chem. B* **2005**, *109*, 22045−22052. (c) Kelly, R. E. A.; Lee, Y. J.; Kantorovich, L. N. *J. Phys. Chem. B* **2005**, *109*, 11933−11939.
(25) Kelly, R. E. A.; Kantorovich, L. N. *J. Phys. Chem. C* **2007**, *111*, 3883−3892.
(26) (a) Sponer, J.; Jurecka, P.; Hobza, P. *J. Am. Chem. Soc.* **2005**, *126*, 10142−10151. (b) Jurecka, P.; Sponer, J.; Cerny, J.; Hobza, P. *Phys. Chem. Chem. Phys.* **2006**, *8*, 1985−1993. (c) Hobza, P.; Sponer, J. *Chem. Rev.* **1999**, *99*, 3247−3276. (d) Sponer, J.; Leszczynski, J.; Hobza, P. *J. Phys. Chem.* **1996**, *100*, 1965−1974.
(27) Ortmann, F.; Schmidt, W. G.; Bechstedt, F. *Phys. Rev. Lett.* **2006**, *95*, 186101.

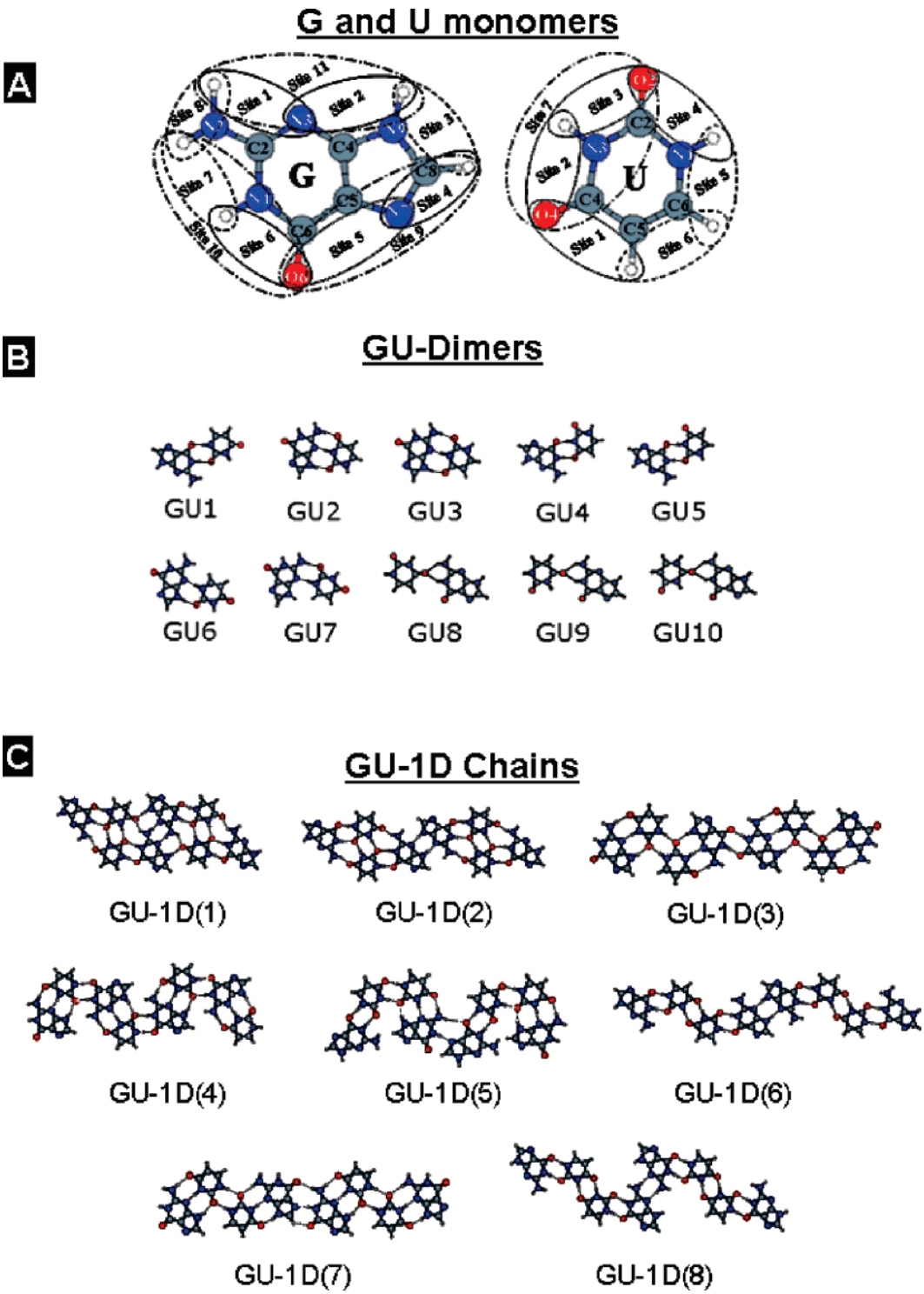

Figure 3. (A) Molecular structures of G and U. Various binding sites which can participate in forming at least double hydrogen bonds between molecules are explicitly indicated.[25] Four types of sites can be identified: (I) two hydrogens (indicated by dashed lines), (II) two acceptors (dotted), (III) one hydrogen and one acceptor (solid), and (IV) three atom sites (dot-dashed). Ab initio DFT calculations of: (B) GU-dimers and (C) GU-1D chains. Note that GU5 is a Wobble base pair, and GU4 is the reverse Wobble base pair.

Pairs are the simplest structures which can be stabilized using these binding sites. Our extensive work on homopairs[24] revealed that the strongest pairs are those containing two hydrogen bonds of either N−H−N or N−H−O types. Figure 3B shows the DFT results for seven most stable GU-dimers (GU1 to GU7), and also some bifurcated pairs (GU8 to GU10). The latter were included here for two reasons: first, due to their presence in other GU crystal structures[28] and also because they form two (nonlinear) N−H−O bonds. The bifurcated pairs are the least stable (−0.30, −0.37, and −0.39 eV, respectively) due to their inability to form linear hydrogen bonds between the monomers. Other pairs have higher stabilities ranging between −0.59 and −0.94 eV, including the GU Wobble base pair GU5 (−0.67 eV) and the reverse Wobble base pair GU4 (−0.76 eV).

(28) Masquida, B.; Westhof, E. *RNA* **2000**, *6*, 9−15.

Table 2. Characteristics of the GU-1D Chain Possibilities[a]

chain	pairs involved in the chain				E_{stab}	|**b**|
GU-1D(1)	$G_6U_4(1)$	$U_3U_3(7)$	U_4G_6 (1)	$G_1G_1(14)$	−3.65	13.4
GU-1D(2)	$G_6U_4(1)$	$U_3U_3(7)$	$U_4G_6(1)$	$G_2G_2(6)$	−3.44	17.5
GU-1D(3)	$G_{11}U_7(2)$	$U_4U_4(1)$	$U_7G_{11}(2)$	$G_6G_6(1)$	−3.37	18.7
GU-1D(4)	$G_6U_4(1)$	$U_7G_{11}(2)$	$G_6U_4(1)$	$U_7G_{11}(2)$	−3.34	16.4
GU-1D(5)	$G_6U_4(1)$	$U_2U_4(2)$	$U_7G_{11}(2)$	$G_7G_5(2)$	−3.20	15.5
GU-1D(6)	$G_6U_4(1)$	$U_2U_2(4)$	$U_4G_6(1)$	$G_1G_1(14)$	−3.12	21.2
GU-1D(7)	$G_{11}U_7(2)$	$U_4U_4(1)$	$U_7G_{11}(3)$	$G_7G_5(2)$	−3.02	19.1
GU-1D(8)	$G_6U_4(1)$	$U_2U_2(4)$	$U_4G_6(1)$	$G_2G_2(6)$	−3.00	17.5
GU-1D(9)	$G_2U_4(6)$	$U_3U_3(7)$	$U_4G_2(6)$	$G_6G_6(1)$	−2.95	18.7
GU-1D(10)	$G_6U_3(5)$	$U_4U_3(3)$	$U_4G_2(6)$	$G_7G_5(5)$	−2.89	15.4
GU-1D(11)[b]	$G_6U_2(4)$	$U_4G_2(6)$			−2.83	10.9
GU-1D(12)	$G_6U_4(1)$	$U_7G_{11}(2)$	$G_6U_3(5)$	$U_7G_{11}(2)$	−2.76	16.4
GU-1D(13)	$G_6U_4(1)$	$U_3U_4(2)$	$U_7G_{11}(2)$	$G_7G_5(2)$	−2.69	16.5
GU-1D(14)	$G_2U_4(6)$	$U_2U_2(4)$	$U_4G_1(7)$	$G_7G_5(2)$	−2.53	21.9
GU-1D(15)	$G_{11}U_7(2)$	$U_4U_4(1)$	$U_3G_6(5)$	$G_5G_7(5)$	−2.43	16.8
GU-1D(16)	$G_6U_3(5)$	$U_4U_2(2)$	$U_4G_2(6)$	$G_7G_5(2)$	−2.38	17.5
GU-1D(17)	$G_6U_3(5)$	$U_4U_4(1)$	$U_3G_6(5)$	$G_2G_2(6)$	−2.38	17.0
GU-1D(18)	$G_6U_3(5)$	$U_4G_2(6)$	$G_6U_3(5)$	$U_4G_2(6)$	−2.30	16.6
GU-1D(19)	$G_6U_3(5)$	$U_4U_4(1)$	$U_3G_6(5)$	$G_1G_1(14)$	−2.01	13.7

[a] The order of stability for each pair is also given within the brackets. The stabilization energies are given in eV and the lattice vectors in Å. [b] GU-1D(11) has only two molecules in the unit cell, so that only two pairs are involved in the chain.

GU-1D Chains. In Figure 3C the eight most stable 1D chains (GU-1D chains) involving the strongest GU1 to GU7 dimer pairs, are shown. A total of 19 chain structures were considered. Their lattice vector magnitudes |**b**| (in Å) and stabilization energies (in eV, include the BSSE correction) are shown in Table 2 in order of their stability (given by the number within the brackets). The specific GU-pairs involved in the bonding are also given, with the binding sites involved in the bonding and the corresponding stability order number in the brackets for that subset.[24,25] As an example, $U_4U_4(1)$ is the most stable UU-dimer where site 4 of one U-molecule joins to site 4 of another U-molecule. An explicit example showing the hydrogen bonding along the chain where dimers are involved is given in Supporting Information **S1** for the chain GU-1D(3).

It should be noted that the bifurcated base pairs GU8 to GU10 in Figure 3 were not considered for the construction of 1D chains. It is very likely that such low-stability formations with only one hydrogen acceptor each would only be metastable because another more stable GU-pair could be formed easily (with little energy input) by rotation around one bond. For instance, rotating the U molecule in GU10 by 180° around the C2−O2 bond (see Figure 3A) results in the most stable pair GU1. Furthermore, the adjacent sites 7 and 6 of G form the strongest bonds with either of the G or U molecules. Therefore, in the most stable GU dimers, the site 7 from the G monomer, which all bifurcated formations rely upon, would be unavailable for connections with other molecules in the chain.

GU-2D Monolayers. Figure 4 shows eight 2D GU-monolayer structures constructed from the eight most stable GU-1D chains and relaxed using the ab initio DFT method. Apart from the GU-2D(4) monolayer, which has eight molecules in the unit cell, all other structures are based on four-molecule unit cells. The lattice vectors and the energies for the monolayer configurations are given in Table 3. Note that the GU chains which contained the Wobble and/or the reverse Wobble pairs were not considered to form 2D monolayers due to the low relative stabilities of their pairs and 1D chains. Interestingly, it can be seen from Table 3 that only one of the G-U monolayer structures, namely GU-2D(2), has lattice vectors similar to those

Table 3. Characteristics of the GU-2D Monolayer Possibilities in Order of Stability Given within the Brackets: the Stabilization Energy (in eV, Includes the BSSE Correction),[23] Lattice Vector Magnitudes |**b**| and |**a**| (in Å), and the Angle between the Vectors, γ

monolayer	related chain	E_{stab}	|**b**|	|**a**|	g (deg)
GU-2D(1)	GU-1D(7)	−4.12	19.1	11.8	53.5
GU-2D(2)	GU-1D(1)	−3.92	13.4	13.5	84.0
GU-2D(3)	GU-1D(2)	−3.88	17.4	12.4	62.4
GU-2D(4)[a]	GU-1D(4)	−3.76	16.4	22.9	89.8
GU-2D(5)	GU-1D(3)	−3.62	18.8	12.5	59.2
GU-2D(6)	GU-1D(6)	−3.58	20.8	13.5	49.8
GU-2D(7)	GU-1D(5)	−3.48	15.8	11.6	89.7
GU-2D(8)	GU-1D(8)	−3.39	13.4	16.9	62.2

[a] The energy for GU-2D(4), containing eight molecules in the unit cell, is halved for the ease of comparison with other monolayers containing only four molecules.

observed in the STM images in Figure 2. Moreover, B and C of Figure 2 show some less bright areas along unit cell vector ***b*** which separates the GU cyclic units and can convincingly be related to the location of weak hydrogen bonds between the GU cyclic units along unit cell vector ***a*** (indicated by green arrows in B and C of Figure 2). It is clear from the comparison of the lattice parameters of the selected highly stable structure GU-2D(2) given in Table 3 with the measured ones from Table 1 that it is the most suitable model to explain the STM image of Figure 2B.

Although a slightly more stable gas-phase structure GU-2D-(1) exists (since it is constructed out of a more stable GU-1D-(1) chain), this is definitely not the observed monolayer. This fact emphasizes again our previous observation that gas-phase calculations alone cannot predict in this *particular case* the most favorable structure due to lack of the molecule-surface interaction.

The other two highly stable GU-2D(3) and GU-2D(4) models are also not suitable to explain the observed STM monolayer, due to their extremely different geometries, so that the GU-2D(2) structure seems to be the most feasible one to explain the STM images.

In order to get a better understanding of the mechanism of the formation of such complex structures, high-accuracy quantum mechanical (QM) calculations that include the substrate as well as the solvent molecules involved in the self-assembly process would be desirable. However, such calculations are not currently feasible.

4. Conclusions

In conclusion, we have presented 2D supramolecular nanostructures formed by guanine and uracil nucleobases on the graphite surface. Upon mixing G and U molecules, a self-assembled nanoscale patterned supramolecular structure consisting of GU-cyclic elementary blocks was observed with dimensions between 1 and 1.4 nm. A systematic methodology in which the first seven most stable G-U pairs were used to construct all most stable 1D chains and then 2D monolayer configurations was proposed and used to identify the observed structure. From a comparison between the experimental and theoretical results, we propose a structural model based on the strongest GU-dimer. Two such dimers form a cyclic structure which acts as the fundamental building block of the monolayer, consisting of a parallel arrangement of 1D chains of the cyclic units. The structure is stabilized by strong hydrogen bonding along the

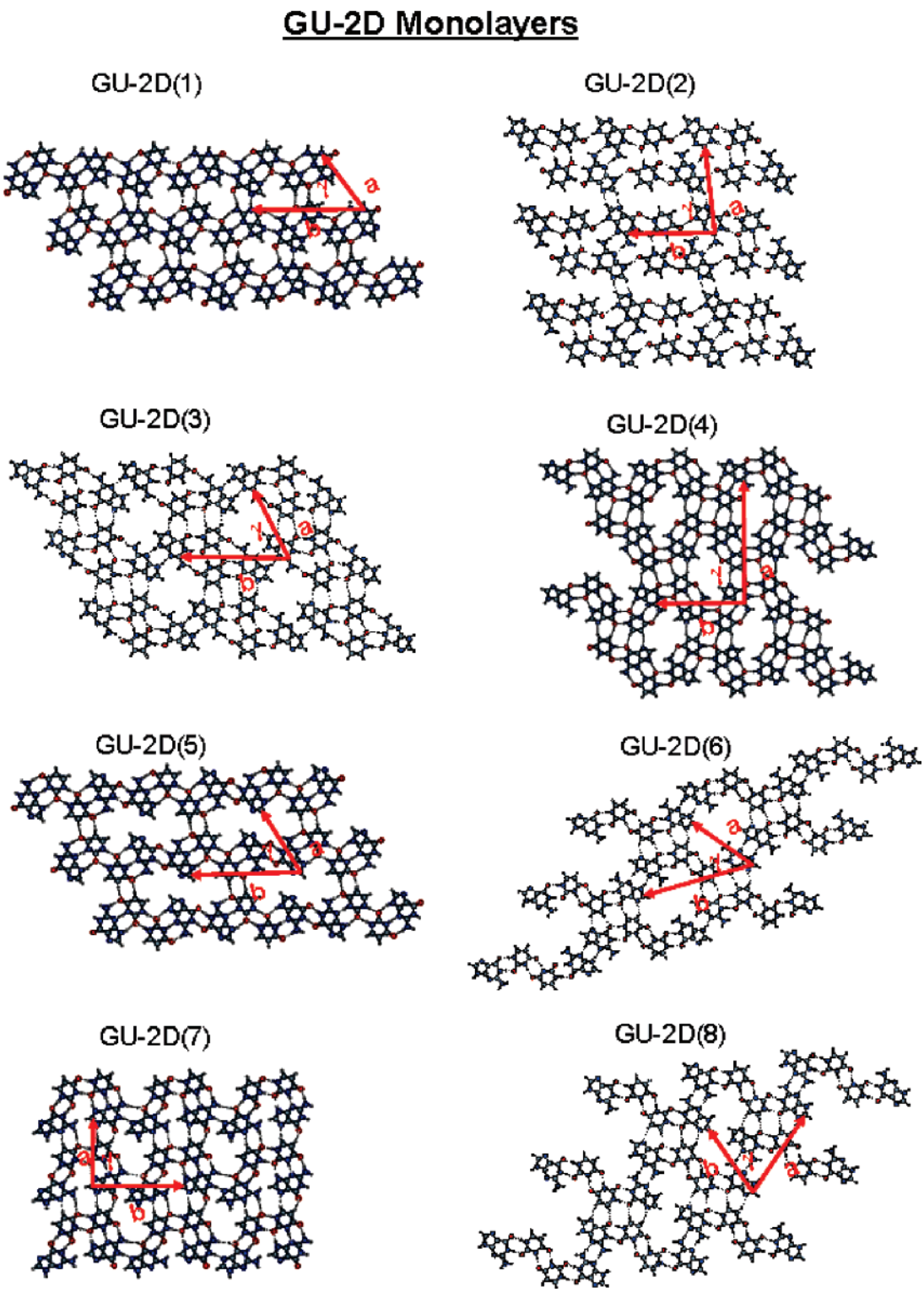

Figure 4. GU-2D monolayers constructed using GU-1D chains of Figure 3C and relaxed by ab initio DFT method. Lattice vectors, ***a*** and ***b***, are indicated in red.

chains and relatively weaker bonding between the chains. This model agrees well with the observed STM images and has high stability. Similar examples of fundamental nanoscale molecular building blocks such as "tetrads" or "quadruplexes" that "consist of either a homo (such as G-quadruplexes), or hetero mixture of DNA bases (such as ATAT-quartets) have been found in biological processes through replication, transcription, and recombination[29] to telomere function. Since it is expected[31] that RNA existed before DNA, a GU assembly may have also played a role as a functional material in the origin of life due to its

(29) Arthanari, H.; Bolton, P. H. *Chem. Biol.* **2001**, *8*, 221−230.
(30) Sowerby, S. J.; Heckl, W. M. *Origins Life Evol. Biosphere* **1998**, *28*, 283−310.
(31) Tanaka, K.; Clever, G. H.; Takezawa, Y.; Yamada, Y.; Kaul, C.; Shionoya, M.; Carell, T. *Nat. Nanotechnol.* **2006**, *1*, 190−194.

importance as an intermediate between form and function in the genetic code.[30] Although the new GU cyclic structures are formed in 2D and not under biological conditions, the dimensions of the pores of these GU structures in the nanometer regime open new opportunities for further progress into host−guest complexation that might be useful, for example, for targeting metal ions.[31]

Acknowledgment. We acknowledge financial support from the Danish Ministry for Science, Technology, and Innovation through the iNANO Center, from the Danish Research Councils. We also acknowledge the computer time on the HPCx supercomputer provided via the Materials Chemistry Consortium. R.E.A.K. is also grateful to the EPSRC for financial support (Grant GR/P01427/01).

Supporting Information Available: An example showing the hydrogen bonding along the chain where dimers are involved for the chain GU-1D(3). This material is available free of charge via the Internet at http://pubs.acs.org.

JA076832F